JTTEE5 15:255-262
DOI: 10.1361/105996306X108192
1059-9630/$19.00 © ASM International

Effect of Deposition Conditions on the Properties and Annealing Behavior of Cold-Sprayed Copper

E. Calla, D.G. McCartney, and P.H. Shipway

(Submitted August 26, 2005; in revised form January 19, 2006)

The deposition of copper by cold gas dynamic spraying has attracted much interest in recent years due to the capability to deposit low-porosity oxide-free coatings. However, it is generally found that as-deposited copper has a significantly greater hardness, and potentially lower ductility, than bulk material. In this article, copper was deposited by cold spraying using helium as the driving gas at both 298 and 523 K. Evidence is presented indicating that the material sprayed at the lower temperature exhibits a lower dislocation density throughout the grain structure than the material sprayed at the higher temperature. The low stacking fault energy of copper restricts recovery during annealing, and thus microstructural changes during annealing only proceed once recrystallization begins. The material sprayed at low temperature (with the low dislocation density) exhibited recrystallization at annealing temperatures as low as 373 K with a corresponding reduction in hardness. However, the copper sprayed with helium at 523 K was resistant to annealing at temperatures up to 473 K where the dislocations in the structure prevented recrystallization. However, at higher temperatures, recrystallization did proceed (with corresponding reductions in hardness). The fracture behavior of the copper that was cold sprayed with helium at 523 K, both in the as-sprayed condition and following annealing, was measured and explained in terms of the annealing mechanisms proposed.

Keywords cold dynamic spraying, heat-treatment of coatings, influence of spray parameters

1. Introduction

Cold gas dynamic spraying (CGDS) is a relatively new spray deposition technique wherein the deposits form due to high-velocity impacts of metallic particles leading to significant plastic deformation and related phenomenon at the deposit-substrate interface and the internal interfaces between the particles themselves (Ref 1-6). These high-velocity impacts lead to significant cold working and in some cases to recrystallization and/or dynamic recrystallization in the deposited material (Ref 6-8). A recent study by Borchers et al. (Ref 8) focused on the microscopic changes in the internal interfaces between the particles in cold-sprayed deposits of a number of face-centered cubic metals, including copper; they described the cold-sprayed copper coating as being nonhomogeneous due to the presence of equiaxed, nanosized grains, elongated nanosized grains, large grains with extremely high dislocation density, and micron-sized grains with recrystallization twins in the absence of dislocations. The nonhomogeneous microstructure of the copper is attributed to its low stacking fault energy, leading to dislocations that are arranged in a dissociated manner, thus hindering cross slip and making recovery difficult (Ref 8-11).

While a number of studies have examined the influence of driving gas temperature on the particle velocity and temperature during cold spraying in terms of features such as deposition efficiency, deposit hardness, bond strength, and porosity (e.g., Ref 12 and 13), there are fewer studies that have examined the influence of the processing conditions on the development of the microstructure. In the present work, copper was sprayed with helium as a driving gas at both 298 and 523 K. The differences in microstructure are revealed by examination of the properties of the as-sprayed materials and their tempering behavior. In addition, the tensile test behavior of the material deposited at the higher temperature is examined both before and after annealing, and is explained in terms of the microstructural features of the materials.

2. Experimental Procedure

2.1 Materials

The powder used for CGDS was commercially pure copper powder (BSA, Birmingham, UK) with a nominal size range of –22 + 5 μm. Coatings were deposited onto 3 mm thick substrates of as-rolled, commercially pure aluminum with a microhardness of 40 kilogram-force (gf)/mm^2 (200 gf load). The substrates were cleaned using methylated alcohol just prior to spraying.

The original version of this paper was published in the CD ROM Thermal Spray Connects: Explore Its Surfacing Potential, International Thermal Spray Conference, sponsored by DVS, ASM International, and IIW International Institute of Welding, Basel, Switzerland, May 2-4, 2005, DVS-Verlag GmbH, Düsseldorf, Germany.

E. Calla, D.G. McCartney, and **P. H. Shipway,** School of Mechanical, Materials and Manufacturing Engineering, University of Nottingham, University Park, Nottingham, NG7 2RD, UK. Contact e-mail: Philip.Shipway@nottingham.ac.uk.

2.2 Cold Gas Dynamic Spraying Deposition and Heat Treatment

Cold gas dynamic spraying was performed with a commercially available system (CGT, Ampfing, Germany) with gas mass-flow controllers. An in-house-designed de Laval nozzle with an area expansion ratio of ~8.6 and a length of 100 mm was used. Coatings were deposited at a constant gas mass flow rate of 2.9×10^{-3} kg/s using helium as the driving gas, both at 298 and 523 K. Pressure and temperature sensors upstream of the nozzle throat measured the pressure (P) and temperature (T) while the system was running. The distance between the nozzle exit and the substrate (the standoff distance) was set to 20 mm, and this was used throughout the experiments. A high-pressure powder feeder (model 1264; Praxair, Danbury, CT) was used to feed the powder to the CGDS gun at 23 g/min using room-temperature helium as a carrier gas. The powder was delivered into a short converging chamber upstream of the throat. The aluminum substrates were placed in a holder for spraying, and the CGDS gun was traversed at a speed of 0.2 m/s relative to the substrates to generate the coating. With the lower gas temperature, six passes were used, resulting in a deposit thickness of ~0.6 mm (more passes resulted in debonding of the deposit under these conditions). In contrast, with the higher gas temperature, 25 passes of the gun were used, resulting in a deposit thickness of ~5 mm. When spraying using the driving gas at 523 K, the substrate temperature was measured using heat-sensitive tapes and was found to be ~373 K.

To examine the effect of heat treatment on the microstructure and properties of cold-sprayed copper, selected deposits were furnace annealed in air for 1 h at temperatures in the range of 373 to 873 K.

2.3 Materials Characterization

A laser granulometer (Malvern Mastersizer; Malvern Instruments, Malvern, UK) was used to determine the powder size distribution. To examine the microstructure of powder particles, they were embedded in cold-setting mounting resin, and ground, polished, and etched using normal metallurgical procedures. Coating cross sections, both as-sprayed and following heat treatment, were also prepared for microstructural examination using similar procedures. Powder and coatings were examined by optical microscopy (OM) both in the unetched condition and following etching using a solution of 5 g of $FeCl_3$ and 5 mL of HCl in 100 mL of ethanol.

Both etched microstructures and fracture surfaces of the tensile test specimens were observed using an FEI XL-30 (Cambridge, U.K.) scanning electron microscope (SEM) operated at 20 kV with secondary electron (SE) imaging.

X-ray diffraction (XRD) analysis of as-sprayed and heat-treated deposits was undertaken using a Siemens D 500 (Bruker-AXS, Coventry, U.K.) powder diffractometer with Cu-Kα radiation. The conditions used were a step size of 0.01° and a counting time of 6 s per step in the 2θ range 40 to 140°.

2.4 Mechanical Testing

The microhardness measurements of the as-sprayed and annealed deposits (sprayed with gas at both temperatures) were carried out on deposit cross sections using a 200 gf load with a LECO (St. Joseph, MI) 400 M microhardness tester. In the case of the material sprayed with driving gas at 523 K, the deposits were thick enough to allow them to be carefully removed from the aluminum substrate and machined using electrical discharge machining to form tensile test samples. The tensile test specimens had a parallel (gauge) length of 30 mm and a width of 6 mm in the gage length, and a thickness of 2 mm. Tensile testing was performed on as-deposited samples as well as on samples annealed at 873 K in a 75% hydrogen-25% nitrogen atmosphere. Tensile samples were also prepared from rolled copper sheet, annealed at 873 K, and tested for comparison with the sprayed material. The tensile tests were performed using a JJ Lloyd (Southampton, U.K.) tensile testing machine with a 30 kN load cell and a crosshead speed of 2 mm/min. Crosshead movement was used as an estimate of sample extension, and the nominal strain was taken as that of the ratio of the crosshead movement to that of the original gauge length.

3. Results

3.1 Powder Characterization

Figure 1 shows both the morphology and the microstructure of the feedstock copper powder. Figure 1(a) shows that the particles have a rounded morphology with only a small fraction exhibiting satellite particles. The etched microstructure (Fig. 1b) shows that the grain size within the powder particles is between 5 and 10 μm. The particle size analysis (Fig. 2) indicates that 87% of the particles are in the specified size range of −22 + 5 μm with approximately 3 vol.% below 5 μm and 10 vol.% above 22 μm.

3.2 As-Sprayed Deposits

Figure 3 shows the etched optical micrographs of as-sprayed material, deposited with the driving gas at the two temperatures used. In both cases, etching has clearly delineated the boundaries between the heavily deformed powder particles. The severe deformation is due to the high strain rate imposed by the impact during cold spraying. Individual grains are not revealed within the particles, in contrast to those clearly observed in the as-received powder (Fig. 1b). In the case of the deposit sprayed with gas at 523 K, the etch has revealed deformation (dislocation) bands within the deposited particles (Fig. 3b); no such deformation bands are seen in the material deposited with gas at the lower temperature (Fig. 3a). Figure 4 shows the XRD patterns of the materials deposited with the driving gas at the two temperatures. In both cases, all of the peaks can be indexed to copper, with no evidence for any other phases (such as copper oxides). It can be observed that in both cases, the peaks exhibit significant broadening, indicating either a fine grain size or the presence of strain in the structure.

3.3 Annealed Deposits

Following annealing at 473 K of the deposit sprayed with helium at 298 K, small recrystallized grains are seen (Fig. 5a). Following annealing at the higher temperature, the grains that are visible are largely in the size range 1 to 5 μm; however, a few

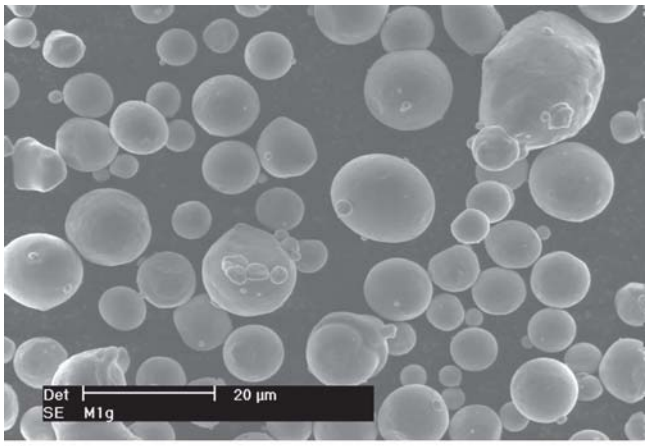

(a)

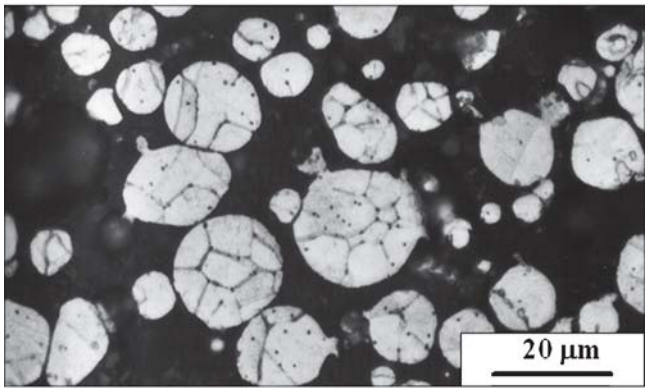

(b)

Fig. 1 Images of the copper feedstock powder: (a) SE-SEM image showing particle morphology; (b) optical image of an etched cross section showing the grain structure within the particles

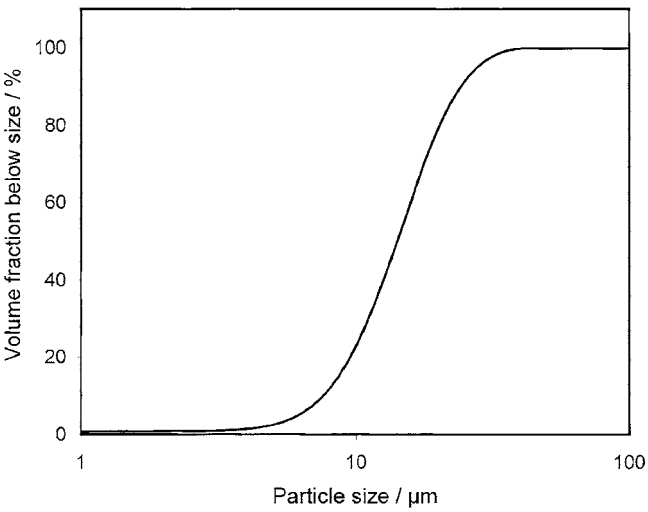

Fig. 2 Particle size distribution of the copper feedstock powder

larger grains on the order of 5 to 10 µm in size are also seen (Fig. 5b). Distinct dark features are visible at particle boundaries that were not observed at the lower annealing temperature. Figure

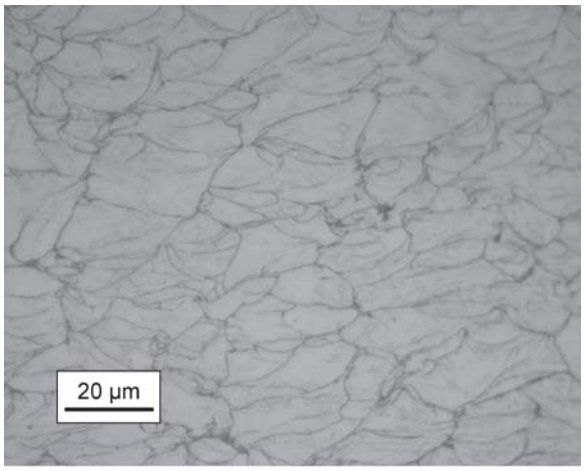

(a)

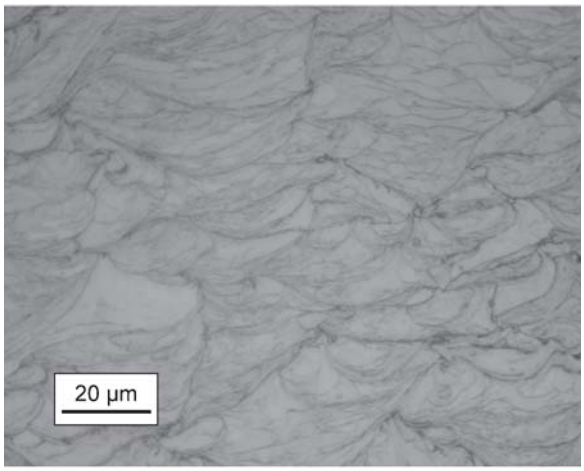

(b)

Fig. 3 OM of cross sections of the as-deposited copper: (a) copper deposited with helium at 298 K; (b) copper deposited with helium at 523 K

5(c) shows an SE-SEM image of the same material as that observed in Fig. 5(b); again, the recrystallized grains are seen, and it is clear that the dark, grain boundary features observed in the OM (Fig. 5b) are indeed porosity (the presence of a grain boundary phase in SE imaging would not be expected to yield such low contrast). Furthermore, energy-dispersive x-ray (EDX) analysis of the dark features revealed only the presence of copper (~100%) with the presence of no other elements (such as oxygen) being detected.

Following annealing at 473 K of the deposit sprayed with helium at 523 K, the boundaries between individual particles are still evident with features at particle boundaries (which are possibly porosity or oxide) and some very fine recrystallized grains; however, the bulk of the structure shows little evidence of recrystallized grains (Fig. 6a). This is very different from the corresponding deposit sprayed with the low-temperature gas (Fig. 5a) where much more evidence for recrystallization is observed. However, following annealing at 773 K (Fig. 6b), recrystallized grains are clearly seen with a recrystallized grain size of 1 to 5 µm. Again, dark features at the particle boundaries are evident,

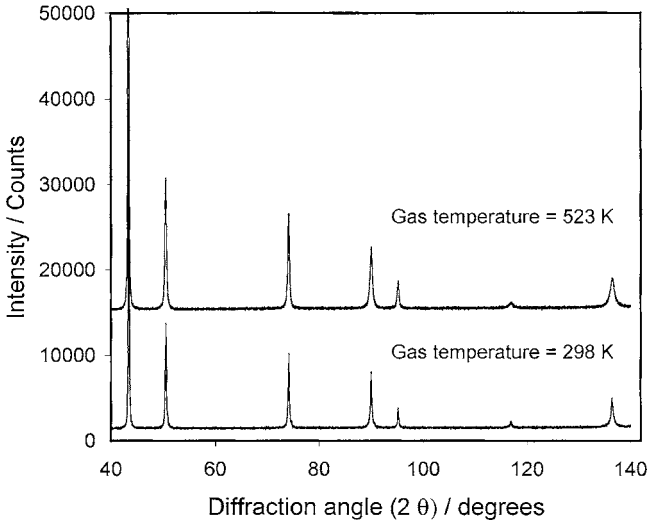

Fig. 4 XRD patterns of the cold-sprayed copper deposits sprayed with helium gas at 298 and 523 K

but these are much less numerous than in the corresponding deposit sprayed with the driving gas at 298 K.

3.4 Mechanical Testing of Deposits

The microhardness of the deposits, sprayed with gas at both 298 and 523 K, both in the as-sprayed condition and following annealing at various temperatures for 1 h is shown in Fig. 7. The microhardness of deposits decreases after annealing; however, the temperature at which the hardness begins to significantly decrease is different in the deposits sprayed using gas at 298 and 523 K.

The deposits formed using driving gas at 523 K had a microhardness of ~179 kgf/mm^2. The hardness of the deposits remained relatively unchanged for annealing temperatures up to 473 K and then decreased when annealed at temperatures of 523 K and above. The deposits exhibited a hardness value of ~90 kgf/mm^2 following annealing at 673 K, and annealing at the higher temperature of 873 K decreased the deposit hardness further to ~65 kgf/mm^2.

The deposits sprayed using driving gas at 298 K had a lower as-sprayed hardness compared with the deposits sprayed using gas at 523 K. In this case, annealing at temperatures as low as 373 K significantly reduced the deposit hardness, and they exhibited a value of ~90 kgf/mm^2 for annealing at 573 K. Annealing at 873 K further reduced the hardness to ~70 kgf/mm^2.

The stress-strain curves obtained from tensile testing of the copper deposited with gas at 523 K, both in the as-sprayed condition and after annealing at 873 K, are shown in Fig. 8. The tensile behavior of the annealed copper sheet is shown in the same figure for comparison. The as-sprayed deposit exhibited a very high tensile strength of 375 MPa but a very small elongation to fracture. An SEM micrograph of the fracture surface of that material is shown in Fig. 9(a); no evidence of ductile fracture is observed, and it seems that fracture has taken place along copper particle boundaries. After annealing the deposit at 873 K, the tensile strength decreased to 230 MPa and elongation to failure increased to around 35%. It is notable that there is little deformation following the attainment of the ultimate tensile strength of the material (Fig. 8). The fracture surface of this ma-

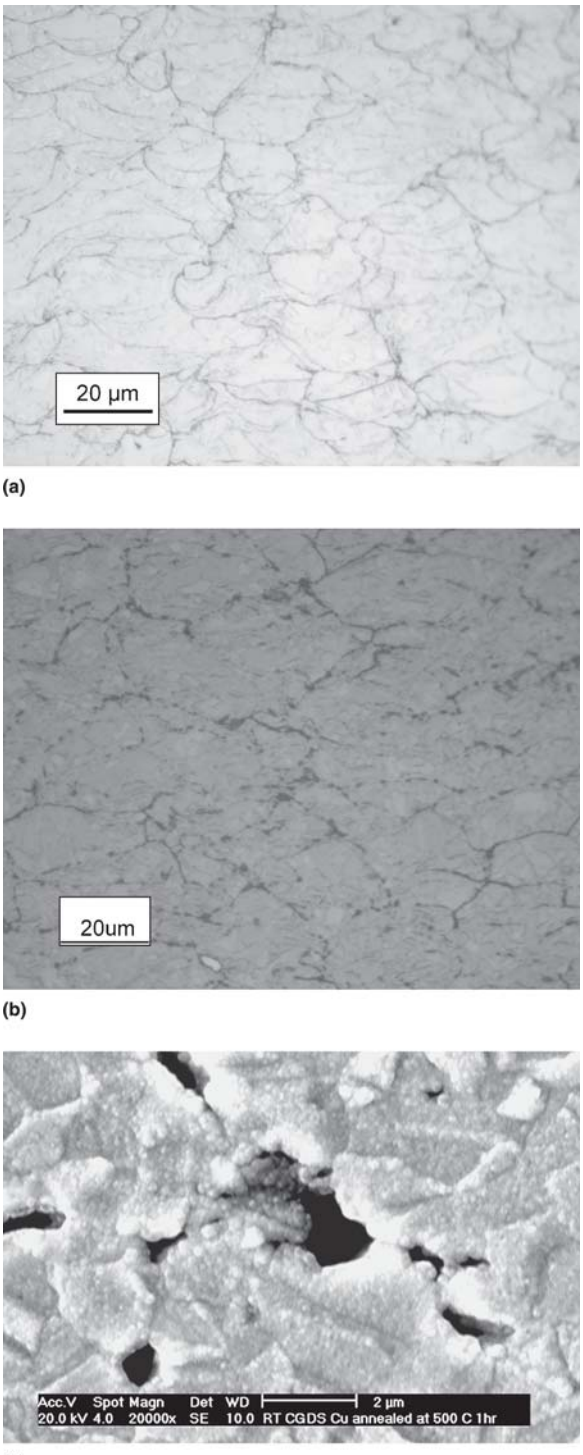

Fig. 5 Images of etched cross sections of copper sprayed with helium at 298 K following annealing: (a) OM following annealing at 437 K; (b) OM following annealing at 773 K; (c) SE-SEM image following annealing at 773 K

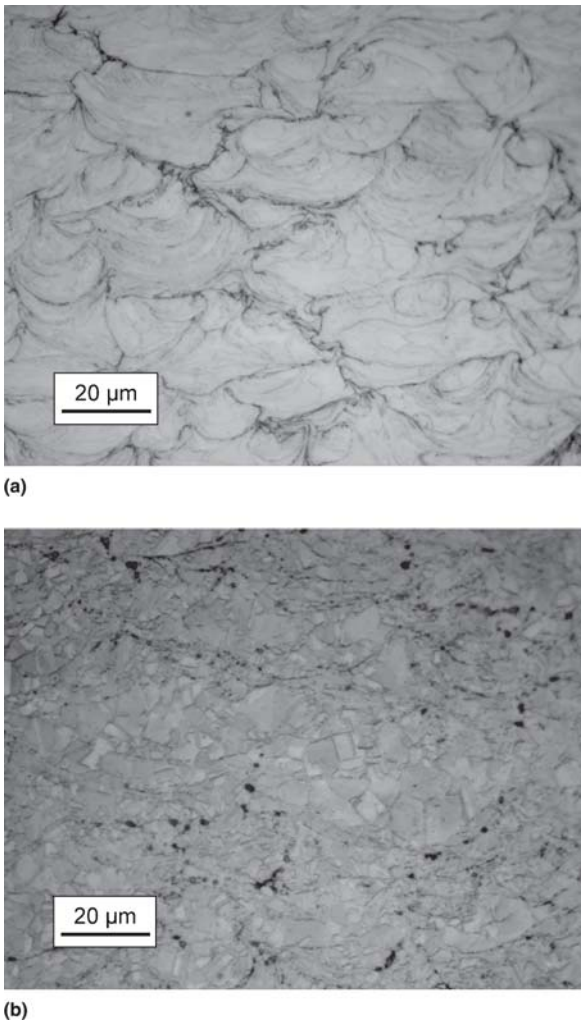

Fig. 6 Images of etched cross sections of copper sprayed with helium at 523 K following annealing: (a) OM following annealing at 437 K; (b) OM following annealing at 773 K

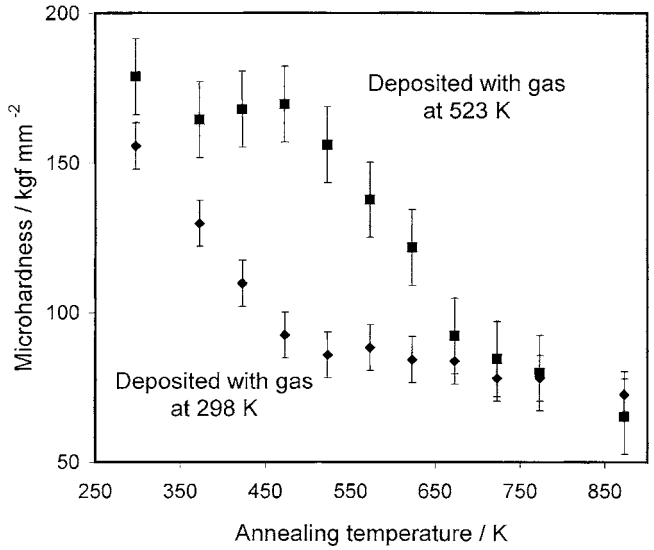

Fig. 7 Microhardness of copper deposits following annealing at 1 h as a function of annealing temperature. Data are shown for deposits sprayed with helium both at 298 and 523 K.

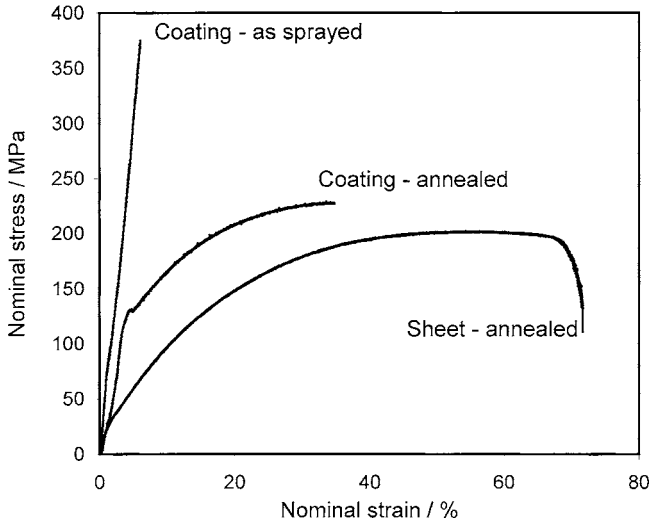

Fig. 8 Tensile behavior of copper sprayed with helium at 523 K in both the as-received state and following annealing at 873 K for 1 h. Tensile data for rolled copper sheet annealed at 873 K for 1 h shown for comparison.

terial is shown in Fig. 9(b) and exhibits features that are characteristic of ductile failure; however, some larger voids are also evident on the fracture surface. The stress-strain curve of the rolled copper sheet following annealing at 873 K shows that the tensile strength of this material was 208 MPa with an elongation to failure of ~71%. Unlike the sprayed material following annealing, the rolled material exhibited significant deformation following the attainment of the ultimate tensile strength.

4. Discussion

4.1 As-Deposited Microstructures

Figure 3 shows the microstructures of the two deposits sprayed with the driving gas at both 298 and 523 K. While both show severe deformation of the original particles and little evidence of porosity, the etched microstructures are qualitatively different, with the material deposited with the higher temperature driving gas exhibiting a higher density of deformation bands throughout the grain structure. Both materials exhibit high values of microhardness, with that of the material deposited with the driving gas at 298 K being 156 kgf/mm^2 while that of the material deposited with the higher driving gas temperature of 523 K was 179 kgf/mm^2. Such high hardnesses in copper are commonly associated with either very fine grain size or high levels of dislocation density; the presence of either one or both of these features in these copper deposits is indicated by the peak broadening in the XRD patterns in Fig. 4. However, this together with the microstructural evidence in Fig. 3 indicates that the material sprayed with the higher-temperature driving gas exhibits a higher dislocation density (in the form of deformation bands) throughout the microstructure.

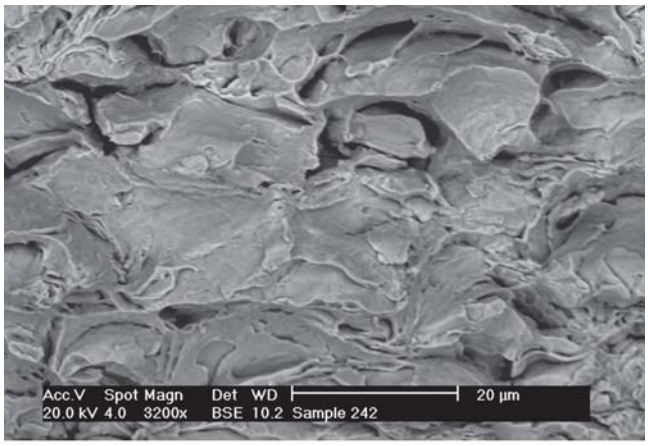

(a)

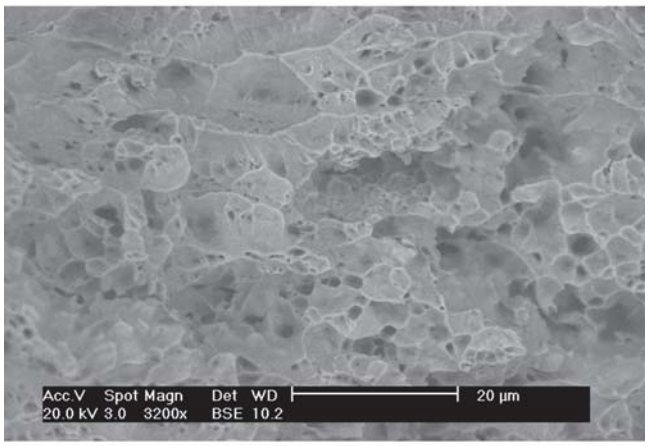

(b)

Fig. 9 SEM images of fracture surfaces of copper deposited with helium at 523 K: (a) tensile tested in the as-deposited state; (b) tensile tested following annealing at 873 K for 1 h

The differences between the microstructures in the two materials will be due to the spraying conditions. Spraying with the higher-temperature gas will result in (a) a higher particle velocity, (b) a higher particle temperature, and (c) a higher substrate temperature. In this work, spraying with the higher-temperature gas (523 K) resulted in a steady-state substrate temperature of ~373 K. In terms of the effect on particle temperature, it must be noted that while the particle temperature increases with the increase of the driving gas temperature from 298 to 523 K, in both cases the particle temperatures at the nozzle exit are expected to be below room temperature; the expansion of the gas in the de Laval nozzle results in a reduction in the gas temperature, and it has been shown that a particle temperature at the nozzle exit of ~200 K would be expected when spraying with helium at 523 K (Ref 14). While the processes controlling the development of the as-sprayed microstructures are not yet fully clear, it is clear that the higher particle velocity resulting from the use of driving gases at elevated temperature will result in higher levels of cold working in such copper deposits.

The microstructure of copper deposited by cold spraying has been investigated in detail by Borchers and colleagues (Ref 6, 8, 15). Transmission electron microscopy has revealed high dislocation densities in cell walls but few dislocations within the cells themselves. However, the current work indicates that the microstructure is sensitive to spraying conditions, and thus it is difficult to compare the work of Borchers et al. (Ref 6, 8, 15) with the current work; Borchers et al. (Ref 6, 8, 15) used nitrogen at 623 K as the driving gas (a nozzle of similar expansion ratio was used in the two pieces of work). The work of Voyer et el. (Ref 14) indicates that the use of nitrogen at such a temperature is likely to result in (a) a particle temperature at the nozzle exit that is perhaps 150 K higher and (b) a particle velocity some 400 m/s lower than that observed when spraying with helium at 523 K.

4.2 Annealing Behavior

The annealing behaviors of the copper sprayed with driving gases at the two temperatures are revealed by the examination of their microstructural development (Fig. 5, 6) and the corresponding hardnesses (Fig. 7). The behavior is consistent with the hypothesis presented earlier, namely, that in the as-sprayed condition the material sprayed with the low-temperature helium exhibits a low dislocation density throughout the grain structure, whereas that sprayed with the helium gas at elevated temperature exhibits a higher dislocation density throughout the grain structure. It is notable that both material types show significant microstructural changes on annealing at elevated temperatures; this is in contrast to copper coatings sprayed from powders with high oxide contents in which the oxide is shown to pin grain boundaries and prevent equiaxing of the structure, even following heat treatment at 993 K for 6 h (Ref 2).

It is known that recovery during annealing is not usually observed in metals such as copper with low stacking fault energy. Thus, in the absence of recovery, the microstructure and mechanical properties of copper are not significantly altered until recrystallization begins (Ref 9). The material sprayed with helium at 298 K exhibits a low dislocation density throughout the grain structure, and as such there is no activation barrier to be overcome for recrystallization to proceed. The substantial reduction in hardness that is observed following annealing at 373 K (Fig. 7) indicates that recrystallization has taken place at this temperature, and the recrystallization is clearly observed by optical microscopy following annealing at 473 K (Fig. 5a). The significant reduction in hardness on annealing at 373 K indicates that the grain structure in the as-sprayed deposit is significantly finer. Annealing at higher temperatures leads to a further reduction in hardness (Fig. 7) resulting from substantial grain growth; following annealing at 773 K, a grain size in the range of 5 to 10 µm is observed (Fig. 5b). It is noticeable that annealing at 773 K resulted in the formation of a large number of voids at preexisting particle boundaries (Fig. 5b and c); the source of these is not clear, but they may have resulted from relaxation of the compressive residual stresses that are developed in these deposits or from the expansion and spheroidization of some of the driving gas (helium) that has been physically trapped within the structure during spraying. Such voids have been observed by McCune et al. (Ref 2) following the annealing of cold-sprayed copper, although it was stated that the mechanism for their formation was not understood. Similar annealing behavior has been observed by Borchers et al. (Ref 15) for copper that was cold sprayed with nitrogen driving gas at 673 K with a signifi-

cant reduction in hardness following annealing at temperatures as low as 373 K. Moreover, in the current work, the hardness of the copper following annealing at 873 K was 72 kgf/mm^2; this compares well with the values for cold-sprayed copper annealed at the same temperature as reported by Borchers et al. (Ref 15).

In contrast to the material sprayed with helium at 298 K, the copper sprayed with helium at 523 K is significantly more resistant to annealing. Up to annealing temperatures of 473 K, no significant reduction in hardness is observed (Fig. 7), and few microstructural changes are observed in the optical microscope (Fig. 6a). This resistance to annealing is again due to the lack of recovery processes operating in copper, which leaves the dislocation network that is present in the as-sprayed material not significantly altered until recrystallization begins (Ref 9). As such, this provides a significant barrier to the recrystallization process. At higher annealing temperatures, new grains are nucleated from the dislocations, and then grain growth occurs. The hardness is observed to drop following annealing at 523 K with a monotonic decrease in hardness as the annealing temperature is raised to 873 K. It is seen that the grain size after annealing at 773 K is in the range of 1 to 5 μm (Fig. 6b), significantly finer than that observed (following annealing at the same temperature) in the copper sprayed at the lower temperature (Fig. 5b). This is again due to the absence of recovery in copper due to its low stacking fault energy, resulting in the dislocations being available for nucleation of new grains, the consequence of which is a large number of smaller-sized grains after recrystallization. The hardness of the copper following annealing at 873 K is 65 kgf/mm^2, which again compares well with the values for cold-sprayed copper that has been annealed at the same temperature as that reported by Borchers et al. (Ref 15).

4.3 Tensile Behavior of Deposits

The tensile behavior was examined only for the copper deposited with helium at 523 K. It can be seen that there was no significant plastic deformation in the as-deposited material and that fracture occurred under a stress of ~375 MPa. Such a stress would not be expected to cause plastic deformation in a material with a hardness of 179 kgf/mm^2. The fracture has occurred primarily along preexisting particle boundaries in the structure (Fig. 9a), and the high strength indicates that the particles themselves were well bonded and were able to support the stress, even along an axis that was perpendicular to the direction of particle impact where it might be expected that interparticle bonding would be weakest.

The tensile testing of deposits annealed at 873 K resulted in a largely ductile failure in the tensile test. This further indicates that there already exists a clean, well-adhered, and largely oxide-free interface between particles in the as-sprayed state, and that annealing the copper deposits at 873 K has resulted in some sintering of the deposited copper particles. The sintering during annealing, along with substantial decreases in strength due to recrystallization result in significantly higher ductility. However, the elongation of the annealed copper deposits is lower than that of the annealed copper sheet; this is due to the presence of pores in the sprayed material following annealing (Fig. 6b), which grow rapidly following the achievement of the ultimate tensile strength and result in failure. These voids can be observed on the fracture surface in Fig. 9(b). In contrast, in the pore-free copper sheet, voids are only nucleated as the ultimate tensile strength is reached and necking starts, resulting in a larger elongation to failure. The ultimate tensile strength of the annealed sprayed copper is ~225 MPa, whereas that of the annealed copper sheet is 200 MPa, a difference of only ~12%. This is in contrast to the hardness values reported by Borchers et al. (Ref 15) where the hardness values of cold-sprayed material annealed at 873 K were ~60% higher than that of copper sheet annealed at the same temperature. The reasons for these differences are not clear.

5. Conclusions

The microstructures developed in copper that were cold sprayed with helium at 298 and 523 K were significantly different. It is proposed that the material sprayed with the higher-temperature driving gas exhibits a higher dislocation density (in the form of deformation bands) throughout the microstructure. The low stacking fault energy of copper restricts recovery during annealing, and thus microstructural changes during annealing only proceed once recrystallization begins. The material sprayed at low temperature (with the low dislocation density) exhibited recrystallization at annealing temperatures as low as 373 K with a corresponding reduction in hardness. However, the copper sprayed with helium at 523 K was resistant to annealing at temperatures up to 473 K with the dislocations in the structure preventing recrystallization. However, at higher annealing temperatures, recrystallization did proceed (with corresponding reductions in hardness). Following annealing at 873 K, the material sprayed at the higher temperature (i.e., the annealing resistant material) exhibited a finer grain size than the material sprayed at the lower temperature, because the high dislocation density in the former material provided a higher free energy for the nucleation of new grains.

The tensile behavior of the material sprayed at the higher temperature revealed strong bonding between particles in the as-deposited material in a direction perpendicular to that of the particle impact vector. In this condition, the high strength of the material resulted in failure by fracture along preexisting particle boundaries at ~375 MPa. Following annealing, the strength decreased substantially with a ductile fracture being observed, indicating that during annealing particle sintering had also occurred. The extension to failure was limited by porosity, which developed during the annealing of the cold-sprayed deposit.

References

1. T. Stoltenhoff, H. Kreye, and H.J. Richter, An Analysis of the Cold Spray Process and Its Coatings, *J. Thermal Spray Technol.,* 2002, **11,** p 542-550
2. R.C. McCune, W.T. Donlon, O.O. Popoola, and E.L. Cartwright, Characterization of Copper Layers Produced by the Cold Gas-Dynamic Spraying, *J. Thermal Spray Technol.,* 2000, **9,** p 73-82
3. R.C. Dykhuizen and M.F. Smith, Gas Dynamic Principles of Cold Spray, *J. Thermal Spray Technol.,* 1998, **7,** p 205-212
4. R.C. Dykhuzien and R.A. Neiser, Optimizing the Cold Spray Process, *Thermal Spray 2003: Advancing the Science and Applying the Technology,* B.R. Marple and C. Moreau, Ed., May 5-8, 2003 (Orlando, FL), ASM International, 2003, p 19-26
5. T. Stoltenhoff, J. Voyer, and H. Kreye, Cold Spraying-State of the Art and Applicability, *International Thermal Spray Conference,* E. Lugscheider and C.C. Berndt, Ed., March 4-6, 2002 (Essen, Germany), DVS Deutscher Verband für Schweißen, 2002, p 366-374

6. C. Borchers, F. Gartner, and T. Stoltenhoff, Microstructural and Macroscopic Properties of Cold Sprayed Copper Coatings, *J. Appl. Phys.,* 2003, **93,** p 10064-10070
7. E. Calla, D.G. McCartney, and P.H. Shipway, Deposition of Copper by Cold Gas Dynamic Spraying: An Investigation of Dependence of Microstructure and Properties of the Deposits on the Spraying Conditions. *Thermal Spray 2004: Advances in Technology and Application,* ASM International, May 10-12, 2004 (Osaka, Japan), ASM International, 2004, p 352-357
8. C. Borchers, F. Gartner, T. Stoltenhoff, and H. Kreye, Microstructural Bonding Features of Cold Sprayed Face Centred Cubic Metals, *J. Appl. Phys.,* 2004, **96,** p 4288-4292
9. P. Cotterill and P.R. Mould, *Recrystallization and Grain Growth in Metals,* Surrey University Press, 1975
10. K. Neishi, Z. Horita, and T.G. Langdon, Grain Refinement of Pure Nickel Using Equal-Channel Angular Pressing, *Mater. Sci. Eng., A,* 2002, **325,** p 54-58
11. S. Komura, Z. Horita, and M. Nemeto, Influence of Stacking Fault Energy on Microstructural Development in Equal-Channel Angular Pressing, *J. Mater. Res.,* 1999, **14,** p 4044-4050
12. D.L. Gilmore, R.C. Dykhuizen, R.A. Neiser, T.J. Roemer, and M.F. Smith, Particle Velocity and Deposition Efficiency in the Cold Spray Process, *J. Thermal Spray Technol.,* 1999, **8,** p 576-582
13. T.H. Van Steenkiste, J.R. Smith, R.E. Teets, J.J. Moleski, D.W. Gorkiewicz, R.P. Tison, D.R. Marantz, K.A. Kowalsky, W.L. Riggs II, P.H. Zajchowski, B. Pilsner, R.C. McCune, and K.J. Barnett, Kinetic Spray Coatings, *Surf. Coat. Technol.,* 1999, **111,** p 62-71
14. J. Voyer, T. Stoltenhoff, and H. Kreye, Development of Cold Gas Sprayed Coatings, *Thermal Spray 2003: Advancing the Science and Applying the Technology,* B.R. Marple and C. Moreau, Ed., May 5-8, 2003 (Orlando, FL), ASM International, 2003, p 71-78.
15. C. Borchers, F. Gartner, T. Stoltenhoff, and H. Kreye, Formation of Persistent Dislocation Loops by Ultra-High Strain-Rate Deformation During Cold Spraying, *Acta Mater.,* 2005, **53,** p 2991-3000